

LASERS

DOI: 10.1070/QEL15974

Laser performance of in-band pumped $Er:LiYF_4$ and $Er:LiLuF_4$ crystals

K.N. Gorbachenya, S.V. Kurilchik, V.E. Kisel, A.S. Yasukevich, N.V. Kuleshov, A.S. Nizamutdinov, S.L. Korableva, V.V. Semashko

Abstract. **Spectroscopic properties of $Er:LiLuF_4$ and $Er:LiYF_4$ crystals in the spectral region near 1.5 μm and the lasing characteristics of these crystals under in-band pumping at a wavelength of 1522 nm are studied. With the $Er:LiLuF_4$ crystal, the maximum slope efficiency with respect to the absorbed pump power was 44% at a wavelength of 1609 nm. Continuous-wave operation of an in-band pumped $Er:LiYF_4$ laser is obtained for the first time. The output power at a wavelength of 1606 nm was 58 mW with a slope efficiency of 21%.**

Keywords: *erbium ions, fluoride crystals, spectroscopy, lasing, in-band pumping.*

1. Introduction

Laser radiation with a wavelength of 1.5–16 μm finds wide application in laser range-finding, ophthalmology, optical location systems and laser-spark emission spectrometry [1, 2]. This radiation can be obtained using solid-state lasers based on active media doped with trivalent erbium ions (Er^{3+}). Radiation in this spectral region is emitted as a result of the transition of Er^{3+} ions from the excited $^4I_{13/2}$ state to the ground $^4I_{15/2}$ state. Previously, due to the absence of efficient sources for pumping erbium media, one used coactivation of these materials with ytterbium ions (Yb^{3+}) absorbing radiation of laser diodes at wavelengths of 0.9–1.0 μm, which, due to the energy transfer between ions, results in the population of the $^4I_{11/2}$ level of erbium with subsequent relaxation to the $^4I_{13/2}$ level. However, these media have some drawbacks. Due to a large (about 40%) difference in the energy of the pump and laser photons, the active element experiences a high thermal load, which restricts the maximum possible pump power. In addition, in these materials, the possibility exists of the reverse energy transfer Er → Yb and the up-conversion transitions from the $^4I_{11/2}$ level of erbium. The appearance of affordable laser diodes based on InGaAsP/InP compounds emitting in the region of 1.5 μm with high spatial and spectral characteristics of the beam [3] stimulated the study of the lasing characteristics of materials doped only with Er^{3+} ions upon in-band pumping directly to the upper $^4I_{13/2}$ laser level [3, 4]. This type of pumping makes it possible to considerably (to below 10%) decrease the Stokes shift and the losses related to up-conversion transitions and reverse energy transfer. In addition, this opens the possibility to study materials with a low efficiency of the energy transfer Yb → Er, such as fluoride crystals.

Previously, lasing under in-band pumping was obtained in various erbium-containing materials, such as garnet [3, 5], vanadate [6–9], sesquioxide [10] and tungstate [11, 12] crystals. The maximum slope efficiency with respect to the absorbed pump power for the $Er:LuVO_4$ crystal pumped by a fibre laser was 64% in the cw regime [8]. An alternative group of materials is the group of fluoride crystals with low phonon energies and, hence, long lifetimes of ions at the $^4I_{13/2}$ level, which ensures significant accumulation of energy in the *Q*-switching regime. Laser operation of in-band pumped fluoride crystals was obtained for the first time in [13] by studying the $Er:LiLuF_4$ crystal. The output power of this laser at a wavelength of 1620 nm under pumping by a fibre laser was 1.24 W with a slope efficiency with respect to the incident pump power of 19%. These results demonstrated that fluoride crystals are promising as matrices for Er^{3+} ions under in-band pumping.

The present work is devoted to the study of the spectroscopic and lasing properties of $Er:LiLuF_4$ (Er:LLF) and $Er:LiYF_4$ (Er:YLF) crystals under the conditions of in-band pumping at the wavelength $\lambda_p = 1522$ nm.

2. Spectroscopy of crystals

The spectroscopic properties of Er:LLF and Er:YLF crystals grown by the Bridgman–Stockbarger method with the Er^{3+} concentration of 1.0 at % were studied using the samples 3.5 mm thick cut so that radiation propagated along the *a* crystallographic axis, which allowed us to record the absorption spectra of the crystals for the π- and σ-polarised radiation. The measurements were performed at room temperature on a Varian CARY-5000 spectrophotometer in the spectral range 1400–1650 nm. The absorption cross section spectra of Er:LLF and Er:YLF crystals are shown in Fig. 1.

The absorption cross section of the Er:LLF crystal at the wavelength $\lambda_p = 1522$ (wavelength of the solid-state laser used in this work as a pump source) is 0.35×10^{-20} and 0.175×10^{-20} cm^2 for the π and σ polarisations, respectively. The Er:YLF crystal is characterised by a similar structure of the absorption spectra. The absorption cross section of the Er:YLF crystal at $\lambda_p = 1522$ nm is 0.34×10^{-20} and 0.22×10^{-20} cm^2 for the π and σ polarisations, respectively.

K.N. Gorbachenya, V.E. Kisel, A.S. Yasukevich, N.V. Kuleshov
Research Centre for Optical Materials and Technologies, Belarusian National Technical University, prosp. Nezavisimosti 65, Bld. 17, 220013 Minsk, Belarus; e-mail: gorby.konstantin@gmail.com;
S.V. Kurilchik, A.S. Nizamutdinov, S.L. Korableva, V.V. Semashko
Kazan (Volga region) Federal University, ul. Kremlevskaya 18, 420008 Kazan, Russia; e-mail: kurilchik.sv@gmail.com

Received 23 November 2015; revision received 11 January 2016
Kvantovaya Elektronika **46** (2) 95–99 (2016)
Translated by M.N. Basieva

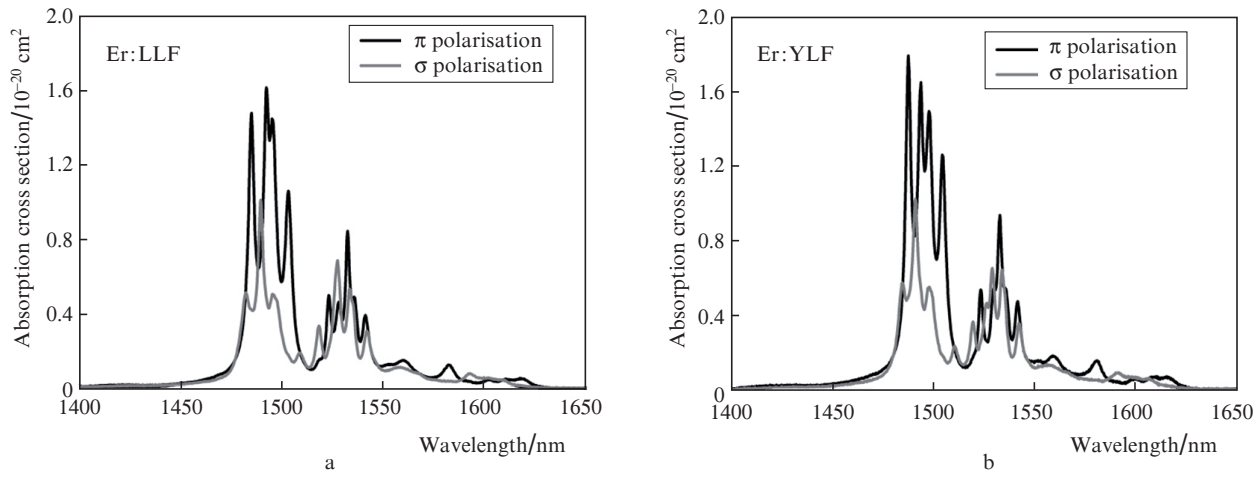

Figure 1. Absorption cross section spectra of (a) Er : LLF and (b) Er : YLF crystals.

The lifetime of the $^4I_{13/2}$ energy level of Er^{3+} ions in the Er : LLF and Er : YLF crystals was determined by measuring the luminescence decay time of suspensions of the crystalline powders by the method described in [14]. As a pump source, we used an optical parametric oscillator based on a BBO crystal with a wavelength of 1530 nm, which was pumped by the second harmonic of a Nd : YAG laser. The excitation pulse duration was 20 ns. The luminescence radiation was separated by an MDR-12 monochromator and recorded by an InGaAs photodiode and a Tektronix TDS3052C digital oscilloscope with a bandwidth of 500 Hz. Assuming that the quantum yield of luminescence corresponding to the $^4I_{13/2} \rightarrow {}^4I_{15/2}$ transition of Er^{3+} ions in fluoride crystals is close to unity, the measured luminescence lifetime can be used as an estimate of the radiative lifetime of the $^4I_{13/2}$ level, which was found to be 10.2 ± 0.5 ms for the Er : LLF crystal and 9.4 ± 0.5 ms for the Er : YLF crystal. These results well agree with data from the literature. In particular, in [15], the radiative lifetime for the Er : YLF crystal was estimated to be approximately 9.4 ms.

The stimulated emission (SE) cross section spectra of the Er : LLF and Er : YLF crystals in the region near 1.5 μm were calculated by two different methods, namely, by the reciprocity method (RM) [16] and the integral reciprocity method (IRM) [17]. The first method is based on the calculation of SE cross sections taking into account the data on the energy level structure of ions in the crystal and the absorption cross section spectra by the formula

$$\sigma_{SE}^{\gamma}(\lambda) = \sigma_{abs}^{\gamma}(\lambda)\frac{Z_1}{Z_2}\exp\left(-\frac{hc/\lambda - E_0}{kT}\right), \quad (1)$$

where σ_{SE}^{γ} and σ_{abs}^{γ} are the SE and absorption cross sections for the γ polarisation; E_0 is the energy gap between the lowest sublevels of the multiplets of the ground and excited electronic states; k is the Boltzmann constant; h is the Planck constant; T is the crystal temperature; c is the speed of light in vacuum; λ is the radiation wavelength in vacuum; and Z_1 and Z_2 are the statistical weight functions of the lower and upper multiplets, respectively, determined as

$$Z_m = \sum_k g_k^m \exp\left(-\frac{E_k^m}{kT}\right). \quad (2)$$

Here, $m = 1, 2$; and g_k^m is the degeneration of the sublevel with the number k and the energy E_k^m measured from the lowest sublevel of the corresponding multiplet. In the calculation, we used data from the literature on the structure of the energy levels of Er : LLF [18] and Er : YLF [19] crystals.

The SE spectra were calculated by IRM using the radiative lifetime of the upper laser multiplet and the absorption cross section spectra. The SE cross sections are calculated by the formula

$$\sigma_{SE}^{\gamma}(\lambda) = 3\exp\left(-\frac{hc}{kT\lambda}\right) \times\left\{8\pi n^2\tau_{rad}c\left[\sum_{\gamma}\int\lambda^{-4}\sigma_{abs}^{\gamma}(\lambda)\exp\left(-\frac{hc}{kT\lambda}\right)d\lambda\right]\right\}^{-1}\sigma_{abs}^{\gamma}(\lambda), \quad (3)$$

where n is the refractive index of the medium and τ_{rad} is the radiative lifetime of the level.

The results of calculations by both methods in one coordinate system for the σ- and π-polarised radiation for the Er : LLF and Er : YLF crystals are shown in Fig. 2. One can see that the spectra are almost identical. This confirms the values of radiative lifetimes of the $^4I_{13/2}$ level of erbium determined from kinetic measurements. For the Er : LLF crystal in the spectral range above 1600 nm, which is characterised by weak absorption, the highest stimulated emission peak for the π polarisation lies at a wavelength of 1619 nm and is 0.31×10^{-20} cm^2. For the σ polarisation, one observes a broad band in the range 1593–1609 nm with cross sections within the range $(0.23–0.30) \times 10^{-20}$ cm^2. For the Er : YLF crystal in the case of the π polarisation, the maximum SE cross section peak lies at a wavelength of 1616 nm and is 0.36×10^{-20} cm^2. The SE band for the σ polarisation with cross sections of $(0.23–0.30) \times 10^{-20}$ см^2 is slightly shifted to the range 1590–1605 nm.

It should be noted that the structure of the determined SE cross section spectra well agrees with the data published in [13], in which the cross sections were calculated by the Füchtbauer–Ladenburg method based on the luminescence spectra [20]. The cross sections determined in that work for the σ polarisation are rather close to our results, while the values for the π polarisation are approximately twofold lower, which, in the case of identical losses for both polarisations, should lead to generation of σ-polarised radiation. However,

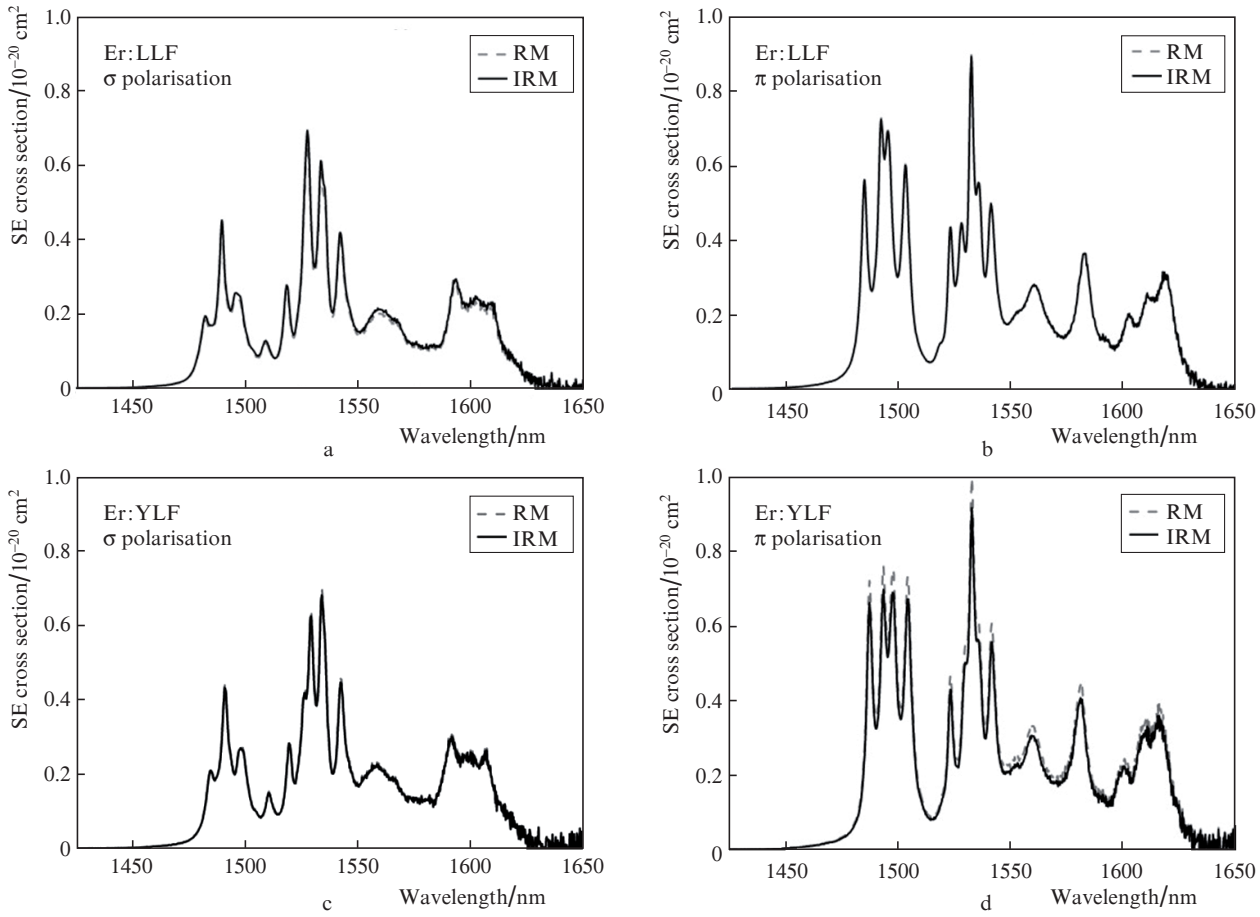

Figure 2. Stimulated emission cross section spectra of (a, b) Er:LLF and (c, d) Er:YLF crystals for the (a, c) σ and (b, d) π polarisations.

the laser radiation in [13] was π-polarised independently of the output mirror transmission. This discordance of the spectroscopic and lasing characteristics is probably caused by errors in the determination of the SE spectra related to the distortions of the luminescence spectra due to the reabsorption of radiation in the sample. The use of RM and IRM with the absorption cross section spectra for both crystals in our work ensures a higher accuracy of determination of SE cross sections.

Based on the absorption and SE spectra, we calculated the gain spectra by the formula

$$g(\lambda) = [\beta\sigma_{SE}(\lambda) - (1-\beta)\sigma_{abs}(\lambda)]N_0, \quad (4)$$

where β is the relative population inversion, which characterises the ratio of ions in the excited state to the total number of ions N_0. The calculated gain spectra for the Er:LLF and Er:YLF crystals are presented in Fig. 3. The horizontal lines show the total loss coefficient α per cavity roundtrip at different output mirror transmissions, which was calculated by the formula [21]

$$\alpha = \frac{1}{2l_a}\left[\ln\left(\frac{1}{1-L}\right) + \ln\left(\frac{1}{1-T_{out}}\right)\right], \quad (5)$$

where l_a is the active medium length, L is the intracavity loss, and T_{out} is the output mirror transmission. The calculation was performed for output mirrors with T_{out} = 1%, 2% and 5%, which we used in laser experiments. The intracavity losses were estimated to be 0.05 and 0.02 for the Er:LLF (l_a = 5.5 mm) and Er:YLF (l_a = 13 mm) crystals, respectively. The use of higher losses for the Er:YLF crystal is explained by the presence of structural microdefects and inclusions in this crystal [22]. The coefficients β were chosen so that the maximum of the resulting gain spectrum $g(\lambda)$ reached the level of the loss coefficient α.

According to the spectra shown in Figs 3a,b, the gain maxima of the Er:LLF crystal lie at wavelengths of 1609 and 1620 nm for the σ and π polarisations, respectively. This determines the laser spectrum in the case of an appropriate output mirror. The gain maxima for the Er:YLF crystal are shifted to shorter wavelengths and are observed at 1606 and 1616 nm for the σ и π polarisations.

3. Laser experiments

The lasing characteristics of the Er:LLF and Er:YLF crystals were studied on an experimental setup, the scheme of which is shown in Fig. 4.

As a pump source, we used an Er:Yb:YAB laser (λ_p = 1522 nm) with the beam quality parameter $M^2 < 1.2$. This laser is described in detail in [23]. The pump radiation was focused by two spherical lenses into a spot with a diameter of 60 μm (at 1/e^2 of intensity) inside the active element, i.e., c-cut Er(1 at %):LLF crystal with a thickness of 5.5. mm or Er (1 at %):YLF crystal with a thickness of 13 mm. This orientation of the crystals allowed us to study the σ-polarised radiation (in [13], the obtained laser radiation of an Er:$LiLuF_4$

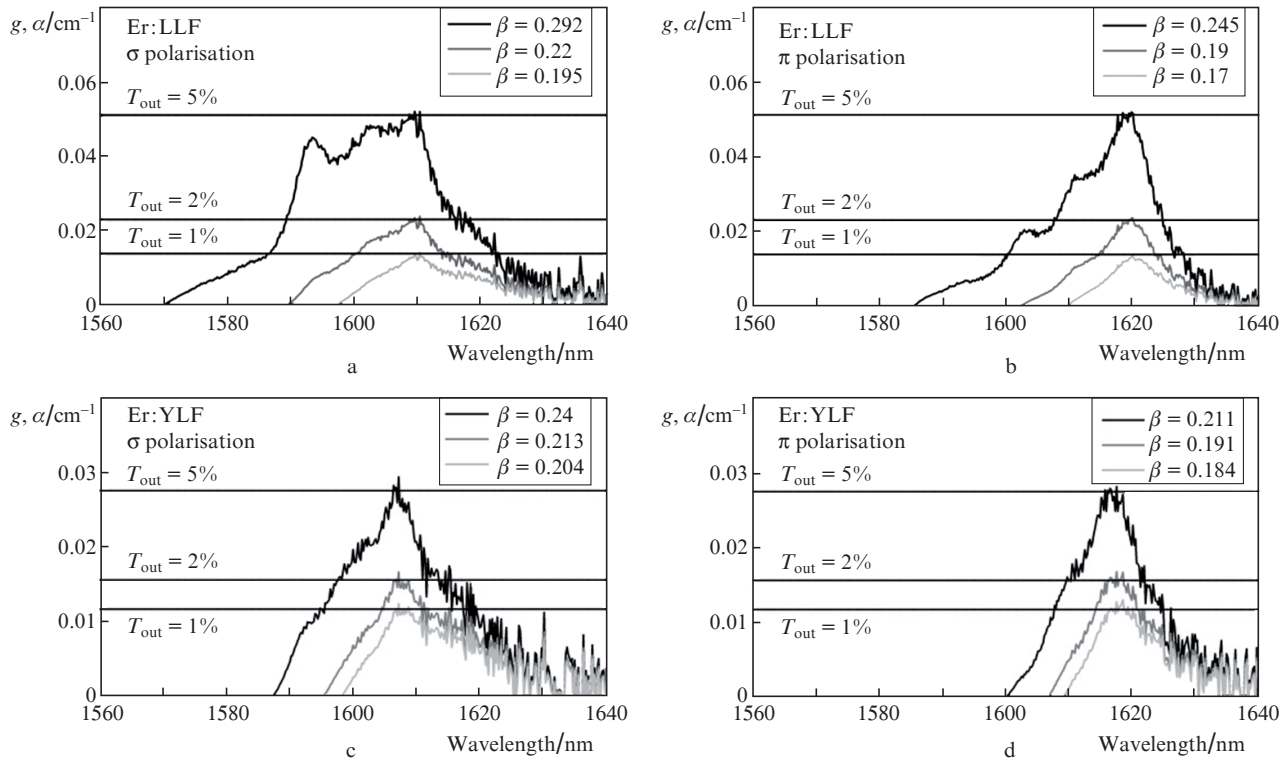

Figure 3. Gain spectra $g(\lambda)$ of (a, b) Er:LLF and (c, d) Er:YLF crystals for the (a, c) σ and (b, d) π polarisations. The straight lines show the levels of total losses at different transmissions of the output mirror T_{out}.

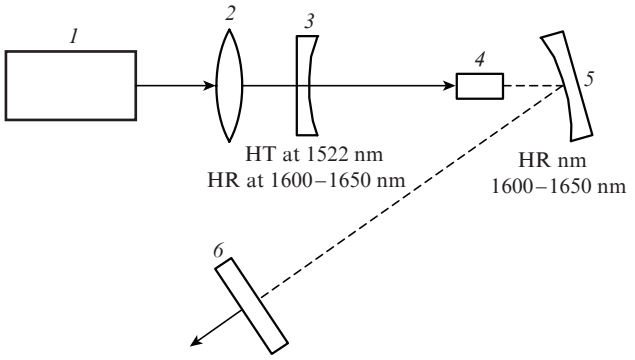

Figure 4. Laser scheme: (*1*) solid-state laser (λ_p = 1522 nm); (*2*) focusing system; (*3*) input spherical mirror (R = –150 mm); (*4*) active element (Er:LLF or Er:YLF); (*5*) spherical mirror (R = –75 mm); (*6*) output mirror (T_{out} = 1%, 2%, 5%).

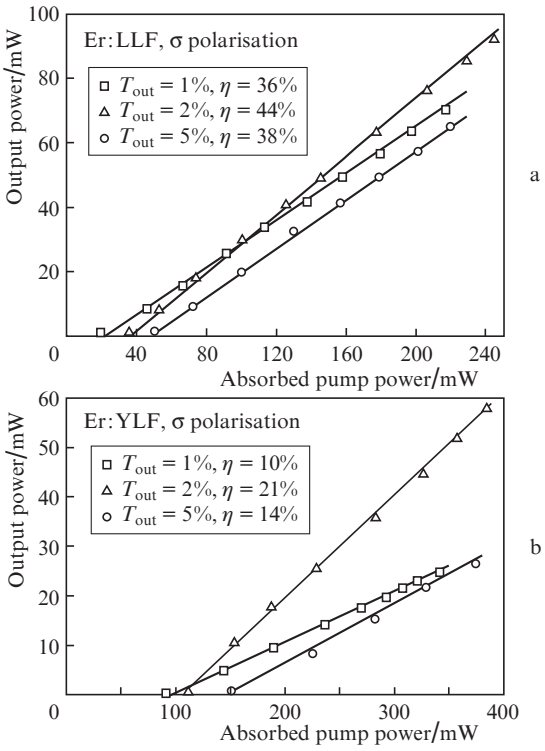

Figure 5. Output characteristics of lasers based on (a) Er:LLF and (b) Er:YLF crystals.

crystal was π-polarised). The faces of both crystals were coated with antireflection dielectric films for the spectral range 1500–1650 nm. The crystals were placed inside the cavity on a copper heat sink without active cooling and were positioned in the focus of a spherical mirror with the curvature radius R = –75 mm. As output mirrors of the cavity, we used plane mirrors with the transmission T_{out} = 1%, 2% and 5% at the lasing wavelengths. The high reflection (HR) coefficient of the output mirrors at the pump wavelength ensured a double pass of the pump beam through the active element.

The obtained output characteristics of the Er:LLF laser are presented in Fig. 5a. The maximum output power P_{out}^{max} and slope efficiency η with respect to the absorbed pump power were 92 mW and 44% and were obtained at the output mirror transmission of 2%. The minimum lasing threshold P_{th} was achieved with a mirror with T_{out} = 1% and was equal to 19 mW. The laser wavelength λ_{gen} was 1609 nm and did not

depend on the output mirror transmission, which corresponds to the results shown in Fig. 3a.

The use of the Er : YLF crystal as an active laser medium allowed us to obtain for the first time cw lasing under in-band pumping. The output characteristics of a laser based on the Er : YLF crystal are shown in Fig. 5b.

Similar to the case of the Er : LLF crystal, the maximum output parameters were achieved at T_{out} = 2%. The maximum output power and slope efficiency with respect to the absorbed pump power were 58 mW and 21%. The minimum lasing threshold, which was achieved at T_{out} = 1%, was 88 mW. The radiation wavelength was independent of the output mirror transmission and was equal to 1606 nm, which corresponds to the results presented in Fig. 3c. The spatial profile of the laser beam in all the experiments was close to Gaussian with $M^2 < 1.2$. The obtained lasing characteristics of the Er : LLF and Er : YLF crystals are listed in Table 1.

Table 1. Lasing characteristics of Er : LLF and Er : YLF crystals.

Crystal	T_{out} (%)	P_{th}/mW	η (%)	P_{out}^{max}	λ_{gen}/nm
Er : LLF	1	19	36	70	1609
	2	35	44	92	
	5	52	38	65	
Er : YLF	1	88	10	25	1606
	2	112	21	58	
	5	150	14	27	

4. Conclusions

The spectroscopic and lasing characteristics of LLF and YLF fluoride crystals doped with Er^{3+} ions are studied. The absorption and stimulated emission cross section spectra in the range of 1400–1650 nm are calculated, the lifetimes of the upper energy level $^4I_{13/2}$ are determined, and the gain spectra are calculated. Continuous-wave σ-polarised laser radiation is obtained for both crystals under in-band pumping at 1522 nm. The maximum output power (92 mW) and slope efficiency with respect to absorbed pump power (44%) are achieved for the Er : LLF crystal at a wavelength of 1609 nm. Lasing of the Er : YLF crystal under in-band pumping is achieved for the first time. The output laser power was 58 mW at a slope efficiency of 21% and a wavelength of 1606 nm.

Acknowledgements. This work was supported by a grant from the Russian Federation Government to the Kazan (Volga region) Federal University (Agreement No. 02.A03.21.0002) and by a grant to the Kazan (Volga region) Federal University for the project part of the state research task in the sphere of scientific activities. The growth of fluoride crystals was supported by the Russian Scientific Foundation (Project No. 15-12-10026).

References

1. Wulfmeyer V., Wizemann H.-D., Schiller M., Fechner M., Huber G. *Proc. 24th Int. Laser Radar Conf.* (Boulder, Col., USA, 2008) SOIP-22.
2. Myers M.J., Myers J.D., Sarracino J.T., Hardy C.R., Guo B., Christian S.M., Myers J.A., Roth F., Myers A.G. *Proc. SPIE Int. Soc. Opt. Eng.*, **7578**, 75782G (2010).
3. Garbuzov D., Kudryashov I., Dubinskii M. *Appl. Phys. Lett.*, **86**, 131115 (2005).
4. Tolstik N.A., Troshin A.E., Kurilchik S.V., Kisel V.E., Kuleshov N.V., Matrosov V.N., Matrosova T.A., Kupchenko M.I. *Appl. Phys. B*, **86**, 275 (2007).
5. Young Y.E., Setzler S.D., Snell K.J., Budni P.A., Pollak T.M., Chicklis E.P. *Opt. Lett.*, **29**, 1075 (2004).
6. Ter-Gabrielyan N., Fromzel V., Ryba-Romanowski W., Lukasiewicz T., Dubinskii M. *Opt. Lett.*, **37**, 1151 (2012).
7. Brandt C., Matrosov V., Petermann K., Huber G. *Opt. Lett.*, **36**, 1188 (2011).
8. Ter-Gabrielyan N., Fromzel V., Yan Z., Han X., Zhang H., Wang J., Dubinskii M. *Opt. Mater. Express*, **4**, 1355 (2014).
9. Gorbachenya K.N., Kisel V.E., Yasukevich A.S., Matrosov V.N., Tolstik N.A., Kuleshov N.V. *Zh. Prikl. Spektr.*, **82**, 214 (2015).
10. Brandt C., Tolstik N.A., Kuleshov N.V., Petermann K., Huber G. *ASSP Conf. 2010* (San Diego, Cal.: OSA, 2010) AMB 15.
11. Fromzel V., Ter-Gabrielyan N., Serrano M.D., Lahera D.E., Cascales C., Zaldo C., Dubinskii M. *ASSP Conf. 2012* (San Diego, Cal.: OSA, 2012) IW3D.
12. Gorbachenya K.N., Kisel V.E., Yasukevich A.S., Pavlyuk A.A., Kuleshov N.V. *Laser Phys.*, **23**, 125005 (2013).
13. Moglia F., Brandt C., Huber G. *ASSP Conf. 2012* (San Diego, Cal.: OSA, 2012) AM4A.
14. Sumida D. *Opt. Lett.*, **19**, 1343 (1994).
15. Payne S.A., Chase L.L., Smith L.K., Kway W.L., Krupke W.F. *IEEE J. Quantum Electron.*, **28**, 2619 (1992).
16. McCumber D.E. *Phys. Rev. A*, **136**, 954 (1964).
17. Yasukevich A.S., Shcherbitskii V.G., Kisel V.E., Mandrik A.V., Kuleshov N.V. *Zh. Prikl. Spektr.*, **44**, 187 (2004).
18. Kaminskii A.A. *Phys. Stat. Sol. (A)*, **97**, K53 (1986).
19. Jayasankar C.K. *Phys. Stat. Sol. (B)*, **155**, 559 (1989).
20. DeLoach L.D., Payne S.A., Chase L.L., Smith L.K., Kway W.L., Krupke W.F. *IEEE J. Quantum Electron.*, **29**, 1179 (1993).
21. Siegman A.E. *Lasers* (Sausalito : Univ. Sci. Books, 1986).
22. Dubinskii M.A., Semashko V.V., et al. *Laser Phys.*, **3**, 480 (1994).
23. Gorbachenya K.N., Kisel V.E., Yasukevich A.S., Maltsev V.V., Leonuk N.I., Kulsehov N.V. *ASSL Conf. 2014* (Shanghai, China: OSA, 2014) AM2A.5.